

Oscillations of factorial cumulants to factorial moments ratio from an eikonal approach

P. C. Beggio^{a,b}

^a *Universidade Federal do Rio Grande do Sul - UFRGS,
Porto Alegre - RS, Brazil.*

^b *Universidade Estadual do Norte Fluminense Darcy Ribeiro - UENF,
Campos dos Goytacazes - RJ, Brazil.*

Abstract

We study the factorial moments (F_q), the factorial cumulants (K_q) and the ratio of K_q to F_q ($H_q = K_q/F_q$) in $pp/p\bar{p}$ collisions using an updated approach, in which the multiplicity distribution is related to the eikonal function. The QCD inspired eikonal model adopted contains contributions of quark-quark, quark-gluon and gluon-gluon interactions. Our work shows that the approach can reproduce the collision energy dependence of the F_q moments, correctly predicts that the first minimum of the H_q lies around $q = 5$ and qualitatively reproduces the oscillations of the H_q moments, as shown in the experimental data and predicted by QCD at preasymptotic energy. The result of this study seems to indicate that the H_q oscillations are manifestation of semihard component in the multiparticle production process. Predictions for multiplicity distribution and H_q moments at the LHC energy of $\sqrt{s} = 14$ TeV are presented.

Key words: Multiplicity distribution, eikonal approach, factorial moments, factorial cumulants.
PACS: 13.85.Hd, 12.40.Ee, 13.85.Ni

1 Introduction

The hadronization mechanism is one of the main problems of QCD [1] and the probability P_n for producing n charged particles in final states (namely multiplicity distribution) is related to the production mechanism of the particles. It also contains information about multiparticle correlations in an integrated form [2] [3] [4]. In the multiparticle production dynamics sector of strong interactions, the multiplicity distribution P_n , its factorial moments F_q and its cumulant moments K_q are relevant physical observables [2] [3]. As pointed out in [5], moment analysis of P_n can also be performed for models as well as for experimental data of hadronic processes. Hence, this approach is common to all processes and methods of analysis. The ratio of factorial cumulants to factorial moments, ($H_q = K_q/F_q$), turns out to be a relevant physical object because, in the framework of perturbative QCD, it was theoretically predicted that the K_q (or equivalently the H_q moments) of P_n should present oscillations in sign as a function of its order q , and that H_q has its first minimum at $q \approx 5$ [6]. The predictions

turned out to be confirmed by experiments in all known high energy processes (e^+e^- , pp , $p\bar{p}$, hadron-nucleus and nucleus-nucleus collisions) [7]. QCD yields results on partons, and not hadrons, and since the partons interactions determine the outcome of collisions with many particles produced, the moments H_q are interesting to study because calculations done at parton (p) level can be directly applied at hadron (h) level in the framework of the Generalized Local Parton Hadron Duality (GLPHD), in which we have $H_q^{(h)} = H_q^{(p)}$ (for details see [3]). However, the QCD has not yet been able to explain satisfactorily the P_n and the formation of hadron from their constituent quarks and gluons. Thus, phenomenological approaches are used as source of information for adequate theoretical developments. In [8], we have update and applied an existing phenomenological approach, referred to as *Simple One String Model - SOSM* [9], which allows simultaneous description of several experimental data from elastic and inelastic channels. This simple model is also able to predict P_n from ISR to Collider energies (30.4 - 900 GeV) without free parameters [10] [11]. In addition, the model allows us to study the inelasticity in $pp/p\bar{p}$ reactions, for which experimental information is scarce [8]. Our goals are to study the collision energy

Email address: beggio@uenf.br (P. C. Beggio).

dependence of F_q moments and investigate whether is possible predict, within the framework of the *SOSM*, the position of the first minimum of the H_q moments and its subsequent oscillations at higher orders, as qualitatively predicted by QCD at preasymptotic energies and, in addition, compare it to the measured data. The plan of the paper is as follows. In Section 2 we briefly discuss the main points of the *SOSM*, as well as their inputs. In the section 3 we present the basic definitions of the multiplicity distribution moments, applying the theoretical framework of the model and computing some moments of the P_n . Results and discussions are in Section 4. The concluding remarks are the content of Section 5.

2 A model for P_n

The main Eqs. of the *SOSM* are

$$\langle n(s) \rangle P_n(s) = \frac{\int d^2b \frac{[1 - e^{-2\chi_I(s,b)}]}{f(s,b)} \psi^{(1)}\left(\frac{z}{f(s,b)}\right)}{\int d^2b [1 - e^{-2\chi_I(s,b)}]}, \quad (1)$$

where

$$f(s, b) = \xi(s) [\chi_I(s, b)]^{2A}, \quad (2)$$

$$\xi(s) = \frac{\int d^2b [1 - e^{-2\chi_I(s,b)}]}{\int d^2b [1 - e^{-2\chi_I(s,b)}] [\chi_I(s, b)]^{2A}}, \quad (3)$$

and

$$\psi^{(1)}(z) = 2 \frac{k^k}{\Gamma(k)} z^{k-1} e^{-kz}. \quad (4)$$

$\psi^{(1)}$ corresponds to the KNO form of the negative binomial distribution (NBD) (or gamma distribution) [12], \sqrt{s} is the center-of-mass energy, $\langle n \rangle$ is the average multiplicity, $z = n / \langle n(s) \rangle$ represents the usual KNO scaling variable, b is the impact parameter, Γ is the usual gamma function, χ_I is the imaginary part of the complex eikonal function and $\xi(s)$ is determined by usual normalization condition on P_n [9]. The main points of the model are summarized as follows:

- (1) $P_n(s)$ has been constructed by summing contributions (multiparticle creation) coming from hadron-hadron collisions taking place at fixed value of b ;
- (2) at each value of b , the multiplicity distribution of the secondaries, $\psi^{(1)}$, is narrow and follows a gamma distribution, which is characterized by the k parameter. The fact that the observed P_n is broad arise from integration over b . There are both empirical and theoretical reasons for the choice of Eq. (4). The form successfully describes the empirical multiplicity distributions in e^+e^- annihilations, yielding the values of A and k parameters adopted in this analysis [9]. Theoretically, the gamma distribution arise as a solution of the QCD evolution equation for three gluon branching [13], which is a

good approximation, since at high energies gluons dominate the parton-parton cross section. More recently NBD has been derived from the Color Glass Condensate approach, which indeed predict the needed NBD [14];

- (3) the energy deposited for particle production, at each b , depends upon the eikonal function in a power law form, [8] [9] [10] [11]

$$\langle n(s, b) \rangle \propto [\chi_I(s, b)]^{2A}. \quad (5)$$

The last Eq. is physically motivated by the fact that the eikonal may be interpreted as an overlap, on the b plane, of two colliding matter distributions [15]. A possible physical picture of *SOSM* is that a process, occurring at fixed value of b , may be interpreted as due to an elementary parton-parton collision, with the formation of an object like a string [10] [11]. Hence, probably one parton-parton pair interaction has triggered the multitude of final particles observed in the interval $30 < \sqrt{s} \leq 900$ GeV. The model permits a calculation of the full phase space P_n , as well as its moments, once the eikonal is given and appropriate values for k and A are adopted. In this work we have kept the choices done in [9], borrowing their results, also used in [8]. Specifically, we have used the values of $k=10.775$ and $A=0.258$ and adopted the QCD inspired complex eikonal determined from elastic channel studies [16], in which the eikonal is written as a combination of an even and odd eikonal terms related by crossing symmetry $\chi_{pp}^{\bar{p}p}(s, b) = \chi^+(s, b) \pm \chi^-(s, b)$. The even eikonal is written as the sum of quark-quark, quark-gluon and gluon-gluon contributions:

$$\chi^+(s, b) = \chi_{qq}(s, b) + \chi_{qg}(s, b) + \chi_{gg}(s, b), \quad (6)$$

while the odd eikonal is parametrized as

$$\chi^-(s, b) = C^- \sum \frac{m_g}{\sqrt{s}} e^{i\pi/4} W(b; \mu^-). \quad (7)$$

The various parameters and functions involved in last two equations are discussed in [16], and the adopted QCD-inspired eikonal satisfies crossing symmetry, analyticity and unitarity [16].

3 Analysis of experimental data

The normalized factorial moments are defined by [12]

$$F_q = \frac{1}{\langle n \rangle^q} \sum_{n=q}^{\infty} n(n-1)\dots(n-q+1) P_n, \quad (8)$$

where $\langle n \rangle = \sum n P_n$ is the average multiplicity and q is a positive integer and represent the order (or rank) of

the moments. The normalized factorial cumulants can be calculated recursively from F_q according to

$$F_q = \sum_{m=0}^{q-1} \frac{(q-1)!}{m!(q-m-1)!} K_{q-m} F_m. \quad (9)$$

In turn, the ratio of factorial cumulants to factorial moments of P_n , are written as

$$H_q = \frac{K_q}{F_q} \quad (10)$$

and should present oscillations in sign as a function of its order q . Some experimental results, used in this work, are given in terms of the reduced C -moments and defined by [12]

$$C_q = \frac{\langle n^q \rangle}{\langle n \rangle^q} = \frac{\sum n^q P_n}{(\sum n P_n)^q}, \quad (11)$$

where q is a positive integer. The normalized C -moments can be expressed through normalized factorial moments F_q and, for the first five moments we have [17]

$$C_2 = \frac{1}{\langle n \rangle} + F_2, \quad (12)$$

$$C_3 = \frac{3C_2}{\langle n \rangle} - \frac{2}{\langle n \rangle^2} + F_3, \quad (13)$$

$$C_4 = \frac{6C_3}{\langle n \rangle} - \frac{11C_2}{\langle n \rangle^2} + \frac{6}{\langle n \rangle^3} + F_4, \quad (14)$$

$$C_5 = \frac{10C_4}{\langle n \rangle} - \frac{35C_3}{\langle n \rangle^2} + \frac{50C_2}{\langle n \rangle^3} - \frac{24}{\langle n \rangle^4} + F_5. \quad (15)$$

The F_q and H_q moments of charged particles at the CERN ISR in pp collisions and of the UA5 Collaboration in $p\bar{p}$ are analyzed by *SOSM*. The Eqs. (1) - (4) have been applied to obtain the theoretical values of P_n . The F_q , K_q and H_q moments were obtained from theoretical and experimental values of P_n according to Eqs. (8) - (10), where the known values of $F_1=K_1=1$ and $F_0=0$ have been used [4]. As mentioned, the model enable us to calculate P_n in full phase space. Thus, at ISR energies (30.4 - 62.2 GeV) and at Collider energy of 546 GeV, we have studied the sample of inelastic events [18] [19], and studied the non-single-diffractive (NSD) experimental data at energies of 200 and 900 GeV since, for the last two energies, P_n have been measured only in NSD $p\bar{p}$ collisions. [20]. The \sqrt{s} dependence of the F_q moments, from both model and experimental data, are compared in Fig. 1. Prediction for F_q at 14 TeV is also presented in Fig. 1. We now turn to calculation of the H_q moments as a function of its order q . The results are shown at ISR energies in Figs. 2-5 and those for the UA5 Collaboration, from 200 to 900 GeV, in Figs. 6-8. For the sake of discussions, we have also plotted the corresponding P_n against n . Theoretical P_n and H_q plots in

full phase space at the LHC energy of $\sqrt{s}=14$ TeV are presented in Fig. 9, in which we have used the value of $\langle n(s) \rangle \simeq 108$ from Ref. [21]. Here, we would like to observe that, at LHC, P_n in pp collisions at $\sqrt{s} = 0.9, 2.36$ and 7 TeV have been measured in different pseudo-rapidity ranges, from $|\eta| < 0.5$ to $|\eta| < 2.4$ [22]. However, the *SOSM* enable us to calculate P_n , and its moments, in full phase space, $|\eta| < 5$. For this reason, comparison of model predictions to LHC data are not presented.

4 Results and discussions

The energy dependence of the F_q can be used to study the KNO scaling hypothesis [12]. The model predicts that for each value of q , F_q increases only slightly over the ISR range, but increases more substantially between the ISR and the CERN Collider, in good agreement with the experiments, indicating that the KNO scaling is approximately valid at ISR, Fig. 1. However, as the energy rises into the CERN Collider and LHC ranges, F_q shows an increase with \sqrt{s} , demonstrating that the KNO scaling is broken. P_n in the Eq. (1) depends on the eikonal and also on the values of A and k parameters, which are fixed numbers ($A=0.258, k=10.775$) in the interval of energy studied. Hence, the model relates the energy dependence of the F_q to that of the eikonal function. Thus, the *SOSM* qualitatively predicts the violation of KNO scaling by changing only the eikonal function, without changing the underlying elementary interaction, in agreement with what could be expected from QCD. This result is qualitatively in agreement with those obtained by CMS Collaboration, albeit in smaller pseudo-rapidity intervals [22] [8]. It seems interesting, since the adopted QCD inspired eikonal, Eqs. (6) - (7), has been determined phenomenologically to give good fits to measurements of elastic channel observables, namely the total cross section (σ_{tot}), the ratio of the real to the imaginary part of the forward scattering amplitude (ρ), and the logarithmic slope of the differential elastic scattering cross section in the forward direction (B) [16]. Concerning the H_q moments, at the energies of $\sqrt{s} = 52.6, 546$ and 900 GeV model predictions are in good agreement with the data up to $q = 16$. Now, at the energies of $\sqrt{s} = 30.4, 44.5$ and 62.2 GeV the data behavior seems theoretically described until $q \approx 13$. At $\sqrt{s} = 200$ GeV there are discrepancies between theoretical and observed points. However, we can see that the theoretical first minimum lies around $q=5$, for all energies studied in this work. At this point we would like to call attention for the interesting results: the *SOSM* qualitatively reproduces the H_q oscillations and correctly predicts the position of the first minimum, in wide interval of energy and with no free parameter, which could be adjusted to achieve agreement with the experimental results. Now, we proceed to a possible interpretation of the H_q oscillations in the framework of *SOSM*. However, it should be noted that the oscillatory observed behavior of H_q 's has one unphysical origin, which is consequence of dealing with

truncated P_n , due to finite statistics of data samples [23]. In the present approach, the even part of the eikonal, Eq. (6), contains quark-quark, quark-gluon and gluon-gluon components, being the eikonal functions $\chi_{qq}(s, b)$ and $\chi_{qg}(s, b)$ needed to describe the lower energy forward data, while $\chi_{gg}(s, b)$ contribution dominates at high energy and determines the asymptotic behavior of cross sections. The rise of the cross section with \sqrt{s} is consequence of the increasing number of gluons soft populating the colliding particles, increasing the probability of perturbative small- x gluon-gluon collisions. The multiparton interactions lead to the appearance of minijets, implying in the semihard contribution in the multiparticle production process, as \sqrt{s} increases. It is also important to note that the eikonal $\chi_{gg}(s, b)$, used by Block et al., is identical to the one used in mini-jet models [16]. Hence, and in view of Eq. (5), the physical picture that emerges is that at relatively lower collision energy, the particle production process is characterized by soft events, receiving contributions from qq , qg and gg scattering events. At high energy, where the $\chi_{gg}(s, b)$ component is predominant, the particle production process is dominated by semihard scattering events, as can be inferred from the increase in the number of gluons populating the incident particles, with the appearance of minijets. Hence, since the general tendency of quite complicated oscillatory behavior of the H_q moments are qualitatively well reproduced by the $SOSM$, it seems quite natural to ascribe it as being manifestations of the semihard component in the multiparticle production mechanism.

5 Concluding Remarks

By using an eikonal approach which allows simultaneous description of several experimental data from elastic and inelastic channels, through unitarity equation in the impact parameter representation, we have analyzed the dependence of the F_q moments as a function of \sqrt{s} , the oscillatory behavior of the H_q moments and the position of its first minimum. Through the specific form of the multiplicity distribution for the secondaries, Eq. (4), a connection is made between the geometric phenomenological approach and the underlying theory of parton branching. It is important to note that the same approach was used to investigate both, the impact parameter and collision energy dependence of the inelasticity in $pp/p\bar{p}$ reactions [8]. Thus, we would like to emphasize the main results from our studies: The approach reproduces the collision energy dependence of the F_q moments, which comes from elastic channel analysis, satisfactorily reproduces the behavior of the H_q moments and correctly predicts the position of the first minimum, in agreement with the predictions from higher order perturbative QCD. From the increase in the content of gluons into protons, leading to appearance of minijets, we have inferred that the oscillatory behavior of the H_q moments are manifestations of the semihard component

in the multiparticle production process. We have shown the consistency between model and QCD results which, from our understanding, is an important step to encourages future improvements in the approach that we have discussed. Thus, in this sense, the present work complements the previous analysis done in [8], since moment analysis of P_n is common to all hadronic processes and methods of analysis [5].

Acknowledgements

I am grateful to E.G.S. Luna for discussions.

References

- [1] Barroso, S.L.C., et al., Nucl. Phys. B (Proc. Suppl.), **75**, (1999) 150.
- [2] A. Giovannini and R. Ugoccioni, Nucl. Phys. B (Proc. Suppl.), **64**, (1998) 68.
- [3] A. Giovannini and R. Ugoccioni, Int. J. Mod. Phys. **A 20**, N 17 (2005) 3897.
- [4] I.M. Dremin and J.W. Gary, Phys.Rep. **349**, (2001) 301.
- [5] I.M. Dremin, Phys. of Atomic Nuclei, **68**, N 5 (2005) 758.
- [6] I.M. Dremin, Phys. Lett. **B313**, (1993) 209; I.M. Dremin and V.A. Nechitaiho, JETP Lett. 51 (1993) 881.
- [7] J. Dias de Deus, C. Pajares and C.A. Salgado, Phys. Lett. **B407**, (1997) 335.
- [8] P.C. Beggio, Nucl. Phys. A, **864**, (2011) 140.
- [9] P.C. Beggio, M.J. Menon and P. Valin, Phys. Rev. **D61**, (2000) 034015.
- [10] P.C. Beggio and Y. Hama, Braz. J. Phys, **37** no. 3B, (2007) 1164.
- [11] P.C. Beggio, Braz. J. Phys, **38** no. 4, (2008) 598.
- [12] Jan Fiete Grosse-Oetringhaus and Klaus Reygers, J. Phys. G: Nucl. Part. Phys. 37 (2010) 083001; hep-ex/0912.0023v1 03/Nov/2009.
- [13] B. Durand and I. Sarcevic, Phys. Lett. **B172**, (1986) 104; Phys. Rev. **D36**, (1987) 2693.
- [14] F. Gelis, T. Lappi and L. McLerran, Nucl. Phys. A, **828**, (2009) 149.
- [15] S. Barshay, Phys. Rev. Lett. 49 (1982) 380.
- [16] M.M. Block, E.M. Gregores, F. Halzen and G. Pancheri, Phys. Rev. **D60**, (1999) 054024-1.
- [17] Michal Praszalowicz, Phys. Lett. **B704**, (2011) 566. **hep-ph/1101.6012v2** 28/Sep/2011;
- [18] ABCDWH Collaboration; A. Breakstone *et al.*, Phys. Rev. **D30**, (1984) 528.
- [19] UA5 Collaboration, G.J. Alner *et al.*, Phys. Rep. **154** ns 5 and 6, (1987) 247.
- [20] UA5 Collaboration, R.E. Ansorge *et al.*, Z. Phys. C - Particles and Fields **43**, (1989) 357.
- [21] S.M. Troshin and N.E. Tyurin, **hep-ph/1106.5317v** 27/Jun/2011;
- [22] CMS Collaboration, hep-ex/1011.5531v1 24/Nov/2010; **JHEP 01** (2011) 079.
- [23] R. Ugoccioni, A. Giovannini and S. Lupia, Phys. Lett. **B342**, (1995) 387.

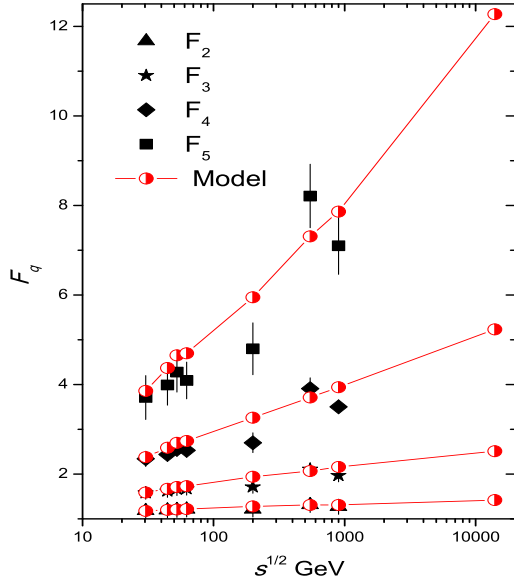


Fig. 1. Normalized factorial moments as a function of the collision energy. At energies of $\sqrt{s} = 200$ and 900 GeV the data points are from NSD events [20]. At other energies the data are from inelastic events [18] [19]. Prediction for F_q at $\sqrt{s} = 14$ TeV is presented. The lines are drawn only as a guidance of the theoretical points.

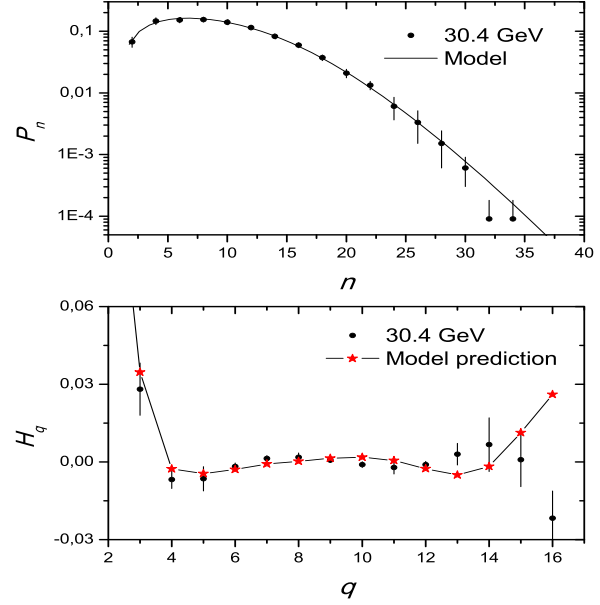


Fig. 2. Theoretical and experimental plots of P_n against n and H_q as a function of its order q for pp at ISR energy. Data points are from [18] and the lines are drawn only as a guidance ($n=2$ to 34).

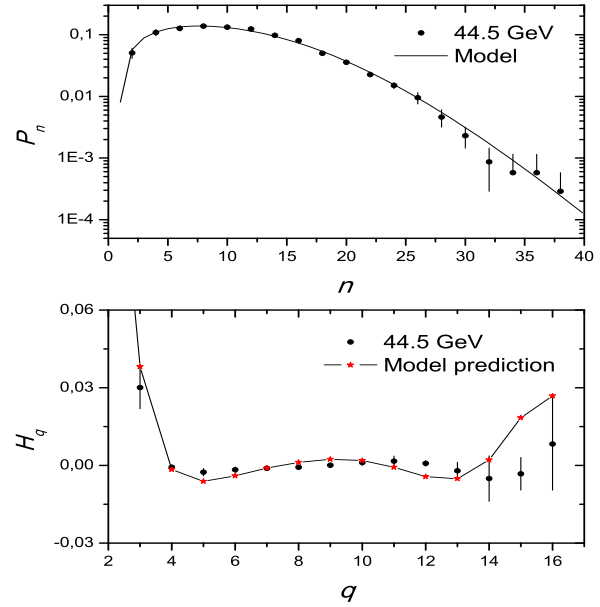


Fig. 3. Theoretical and experimental plots of P_n against n and H_q against q for pp at ISR energy. Data points are from [18] and the lines are drawn only as a guidance ($n=2$ to 38).

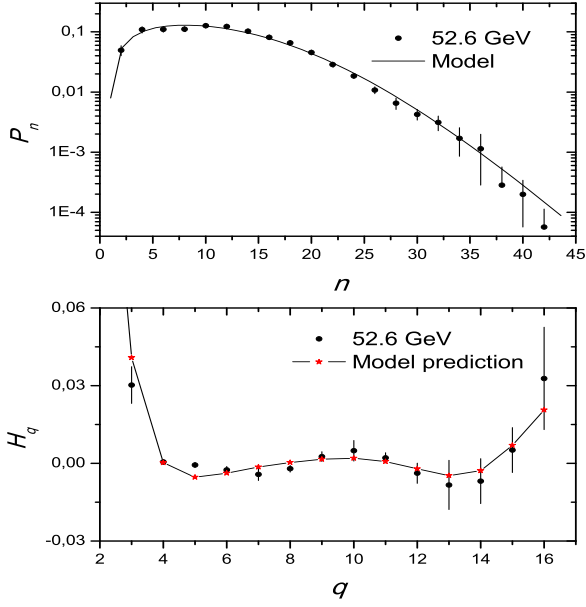


Fig. 4. Theoretical and experimental plots of P_n against n and H_q against q for pp at ISR energy. Data points are from [18] and the lines are draw only as a guidance ($n=2$ to 42).

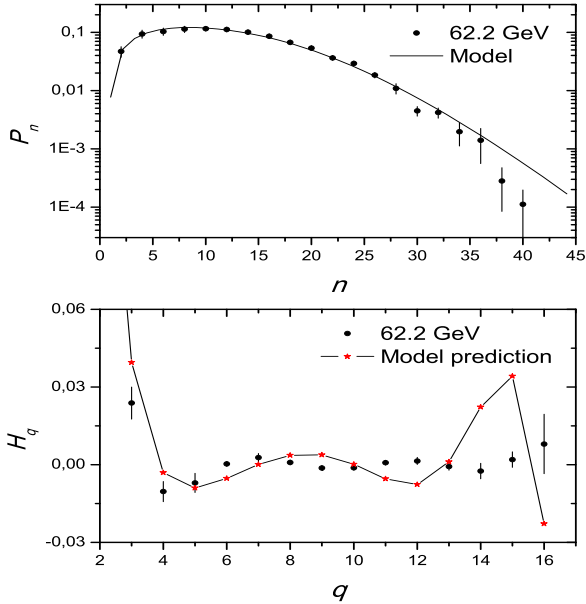


Fig. 5. Theoretical and experimental plots of P_n against n and H_q against q for pp at ISR energy. Data points are from [18] and the lines are draw only as a guidance ($n=2$ to 40).

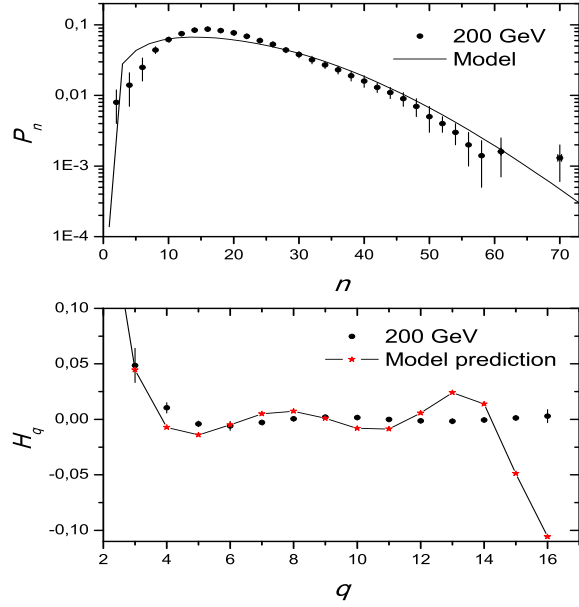


Fig. 6. Theoretical and experimental plots of P_n against n and H_q against q for $p\bar{p}$ at Collider energy. Data points are from [20] and the lines are draw only as a guidance ($n=2$ to 70).

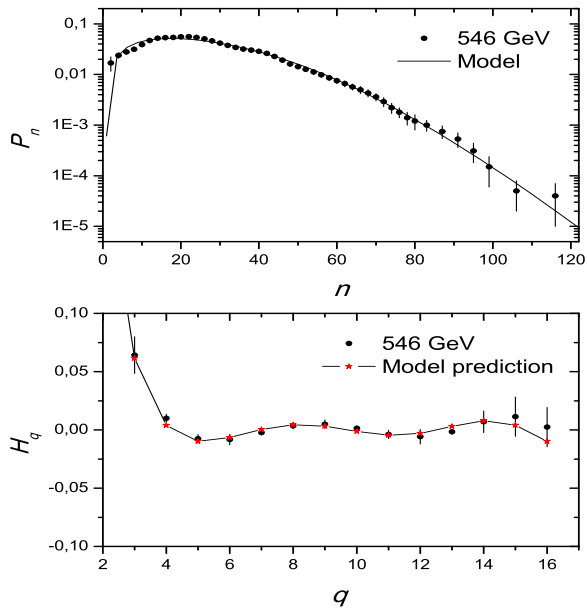


Fig. 7. Theoretical and experimental plots of P_n against n and H_q against q for $p\bar{p}$ at Collider energy. Data points are from [19] and the lines are draw only as a guidance ($n=2$ to 116).

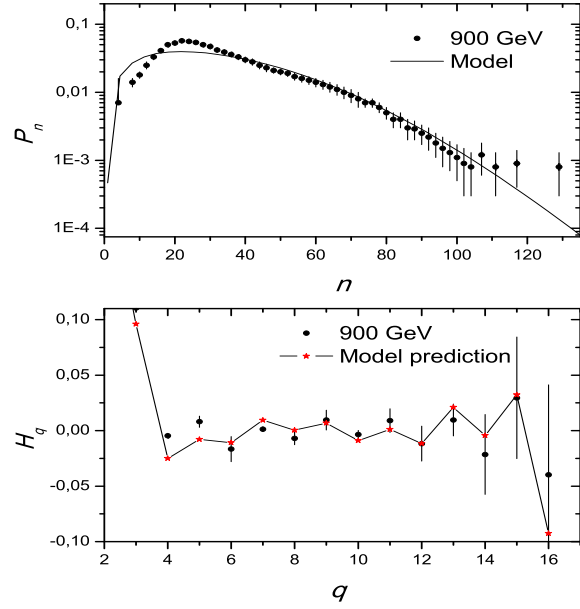


Fig. 8. Theoretical and experimental plots of P_n against n and H_q against q for $p\bar{p}$ at Collider energy. Data points are from [20] and the lines are draw only as a guidance ($n=4$ to 129).

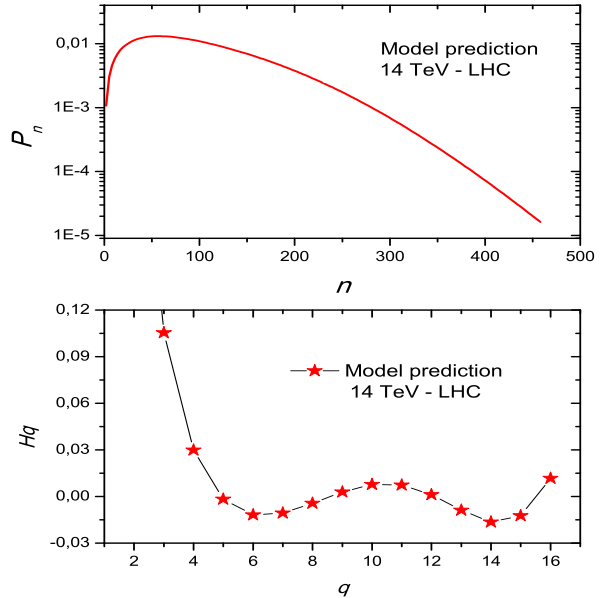


Fig. 9. Theoretical plots of P_n against n and H_q against q for pp at LHC energy. The line is draw only as a guidance ($n=4$ to 350).